# ALIGNMENT STUDY OF AN ELECTRONIC DISTANCE MEASURING INSTRUMENTS CALIBRATION BASELINE USING TOTAL STATION

Isaac Ramos Junior[1], Andrea de Seixas[2], Sílvio Jacks dos Anjos Garnés[3]
[1,2,3] Department of Cartographic Engineering, Federal University of Pernambuco, 50670-901, Recife, Brazil
[1] isaac.ramos@ufpe.br
[2] andrea.seixas@ufpe.br
[3] silvio.jacks@ufpe.br

***ABSTRACT***

*This article examines the alignment of an electronic distance measuring instrument calibration baseline at the Recife campus of the Federal University of Pernambuco, Brazil. The baseline consists of seven pillars equipped with a forced centering device labeled P1 to P7. Pillars P1 and P7 serve as the endpoints for the alignment, with the remaining pillars positioned in between. Data collection was performed using a Topcon GT-605 robotic total station, by the radiation method. Subsequently, the collected data was transferred to a computer and processed with a Python-based program. To delve into the results further, precision estimates were computed. The analysis revealed minor differences in alignment among the pillars, but P2, P4, P5, and P6 exhibited values exceeding the nominal precision of the equipment, that is +/- 2 mm +2ppm. Furthermore, the study indicated that the slight misalignment opens up the possibility of treating the base as a closed traverse in future surveys, such as that formed by pillars P1, P3, P4, P7, P6, P5, P2, P1, opening the way to numerous opportunities of future research.*

***KEYWORDS:*** *Geodetic Engineering, Metrology, Precise Instrumentation.*

## I. INTRODUCTION

The contemporary total station serves as a comprehensive surveying tool, integrating an electronic theodolite, an electronic distance measuring instrument (EDMI), and capabilities for data recording and computation. By combining these features into a singular device, the instrument facilitates the swift and precise 3D positioning of points. These advanced total stations, particularly those at the higher end, may include robotic capabilities [1,2], which incorporate several extra functionalities (such as motion control actuators, cameras, tracking software, etc.), allowing them to function autonomously by executing pre-loaded measurement programs or responding to remote commands [3].

Regarding application, robotic total stations are considered to be in the category of the single point measurement instruments, that is, that collect a single point at a time. However, even though it takes longer, data collection has a value of just a few millimeters of precision, making it among the most accurate in engineering applications [4].

Alignment surveys are widely applicable in engineering, spanning various sectors such as tooling and deformation measurements of extensive engineering structures. Nevertheless, specific applications may demand distinct specialized tools. Practical methods can be categorized based on the approach to establishing the reference line. In this context, conventional surveying techniques, that include triangulation, trilateration, combined triangulation and trilateration, traversing, intersection, and resection where a reference line is defined by two coordinate points, are commonly employed [5].

One kind of structure that needs to be aligned is the EDMI calibration baselines. Comprising two or more stable geodetic monuments, a calibration baseline involves conducting measurements with precise instruments to determine the absolute value of the resultant measurement. The precise calibration of

this baseline allows for the comparison of the precision performance of various types of geodetic instruments [6].

Works relating to the use of total stations precision surveying have been published in the most varied forms. Thus, [7] investigated the effect of battery capacity on the accuracy of Total Stations, as well as the effect of the angle of incidence on the reflecting surface for different colors and types, while [8] added the study of the influence of LASER beam size divergence. Furthermore, [9] studied the determination of a correction equation for the error in prismless distance measurements at a distance of 100 meters, due to the change in the angle of incidence; [10] (2015) investigated the accuracy of observations with a prismless Total Station during the process of monitoring and implementing engineering structures, while [11] studied the degree of reliability of prismless measurements applied to the construction of buildings; [12] and [13] incorporated into their studies the investigation of the divergence of LASER beam size from reflectorless Total Stations; [14] studied the monitoring of structures without using a prism, and [15] studied a method for measuring without a prism in tunnels.

Thus, for the current investigation, a EDMI calibration baseline was chosen. It consists of seven pillars (P1, P2, P3, P4, P5, P6 e P7) with a forced centering device, located on the campus of the Federal University of Pernambuco in Recife, Brazil. The measurements were carried out with a Topcon GT-605 robotic total station, utilizing a 360° prism, and employing the radiation method from P1 and P7 pillars with the aim of studying the interpillar alignment.

## II. MATERIALS AND METHODS

The EDMI calibration baseline chosen to conduct this research was established by the Spatial Metrology Laboratory of the Department of Cartographic Engineering, of the Technology and Geosciences Center (CTG), of the Federal University of Pernambuco (UFPE), Brazil [16]. To enhance clarity, the seven pillars of the base were designated with the names P1, P2, P3, P4, P5, P6, and P7. Figure 1 depicts each pillar appropriately labeled for easy identification.


**Figure 1**. Each individual pillar of the EDMI calibration baseline, in February 2024.

A total station is utilized for measuring distances, as well as vertical angles and horizontal directions. An evolution of this instrument is the robotic total station, in which a single operator can conduct all necessary measurements through automatic aiming at a reflector and wireless communication between

the device and its controller, that is stationed at a designated landmark with a reflector, grants complete control over the device when the operator is at a measured point [17].
To conduct the measurements of this paper, a Topcon robotic total station, model GT-605, and a 360° prism, both owned by UFPE, were utilized (refer to Figure 2 and Figure 3, respectively). The equipment has a linear accuracy of ±2mm + 2ppm (parts per million) and an angular accuracy of 5" [18].
The initial step involved selecting the coordinate system. In pursuit of this, the alignment between the first and last pillars (P1 and P7) was designated as the reference alignment. This alignment served as the basis for determining the positions of the remaining pillars if they were to be aligned. Consequently, the *y*-axis of the local coordinate system was established to coincide with the alignment between pillars P1 and P7.

**Figure 2**. The robotic total station used in the measurements, in February 2024.

**Figure 3**. The 360° prism used in the measurements, in February 2024.

The next step involved data collection using the radiation method [19], following this sequence: The equipment was set up at P1 with a backsight at P7, that was the last pillar of the sequence, and data were collected from the additional points (P2, P3, P4, P5, and P6). Then, the equipment was repositioned at P7 with a backsight at P1, the first pillar of the sequence, and data were once again collected from the same set of points (P2, P3, P4, P5, and P6). This resulted in two sets of data that could be compared.
Subsequently, utilizing all the collected data, the radiation method was computed through a program developed in the Python language, because in its current state, this is an excellent language for developing engineering applications [20]. This program employed the equations (1) and (2) above [21]:

$$xp_i = xp_1 + D_{p1pi}sin(\alpha_{p1pi}) = xp_7 + D_{p7pi}sin(\alpha_{p7pi}) \quad (1)$$

$$yp_i = yp_1 + D_{p1pi}cos(\alpha_{p1pi}) = yp_7 + D_{p7pi}cos(\alpha_{p7pi}) \quad (2)$$

In which:
$xp_i$ is the unknown *x* coordinate of pillar *i*;

$yp_i$ is the unknown *y* coordinate of pillar *i*;
$xp_1$ is the know *x* coordinate of pillar P1;
$yp_1$ is the know *y* coordinate of pillar P1;
$xp_7$ is the know coordinate of pillar P7
$yp_7$ is the know coordinate of pillar P7;
$D_{p1pi}$ is the horizontal distance between P1 and Pi;
$D_{p7pi}$ is the horizontal distance between P7 and Pi;
$\alpha_{p1pi}$ is the angle centered at P1, backsight at P7 and foresight at Pi;
$\alpha_{p7pi}$ is the angle centered at P7, backsight at P1 and foresight at Pi.

The final step involved estimating uncertainties, utilizing the special law of propagation of variances [22,23]. The general expressions for this law for the equations (1) and (2) are equations (3) and (4):

$$\sigma_{xp_i} = \sqrt{(\frac{\partial xp_i}{\partial xp1}\sigma_{xp1})^2 + (\frac{\partial xp_i}{\partial \bar{D}_{p1pi}}\sigma_{D_{p1pi}})^2 + (\frac{\partial xp_i}{\partial \alpha_{p1pi}}\sigma_{\alpha_{p1pi}})^2} \quad (3)$$

$$\sigma_{yp_i} = \sqrt{(\frac{\partial yp_i}{\partial yp1}\sigma_{yp1})^2 + (\frac{\partial yp_i}{\partial \bar{D}_{p1pi}}\sigma_{D_{p1pi}})^2 + (\frac{\partial yp_i}{\partial \alpha_{p1pi}}\sigma_{\alpha_{p1pi}})^2} \quad (4)$$

In addition to all the calculations, all the tables that present the results were also generated by the same program mentioned above, in the Python language.

## III. RESULTS AND DISCUSSIONS

When retrieving data from the equipment, the program specifically chose pertinent information for this study, focusing exclusively on horizontal directions and overall horizontal distances. The relevant data can be found in table 1, where (D) means reading in the direct position of the telescope, and (I) means reading in the reverse position of the telescope.

**Table 1.** Raw data collected for P1 and P7 stations.

| Station | Point | Horizontal Direction | Horizontal Distance (m) |
|---|---|---|---|
| P1 | P2 | 00°00’03” (D) | 8.3009 |
| P1 | P2 | 179°59’56” (I) | 8.3009 |
| P1 | P3 | 359°58’53” (D) | 12.7380 |
| P1 | P3 | 179°58’54” (I) | 12.7380 |
| P1 | P4 | 359°58’38” (D) | 45.8650 |
| P1 | P4 | 179°58’36” (I) | 45.8650 |
| P1 | P5 | 00°00’23” (D) | 95.7540 |
| P1 | P5 | 180°00’20” (I) | 95.7540 |
| P1 | P6 | 359°59’41” (D) | 135.2359 |
| P1 | P6 | 179°59’40” (I) | 135.2359 |
| P1 | P7 | 359°59’27” (D) | 167.4939 |
| P1 | P7 | 179°59’26” (I) | 167.4939 |
| P7 | P1 | 00°00’02” (D) | 167.4940 |
| P7 | P1 | 179°59’57” (I) | 167.4940 |
| P7 | P2 | 359°59’56” (D) | 159.1939 |
| P7 | P2 | 179°59’57” (I) | 159.1939 |
| P7 | P3 | 00°00’04” (D) | 154.7549 |

| | | | |
|---|---|---|---|
| P7 | P3 | 180°00’00” (I) | 154.7549 |
| P7 | P4 | 00°00’18” (D) | 121.6288 |
| P7 | P4 | 180°00’13” (I) | 121.6286 |
| P7 | P5 | 359°58’47” (D) | 71.7380 |
| P7 | P5 | 179°58’45” (I) | 71.7380 |
| P7 | P6 | 359°58’50” (D) | 32.2569 |
| P7 | P6 | 179°58’47” (I) | 32.2569 |

Subsequently, the program conducted the initial processing of the raw data independently for stations P1 and P7. This process involved the calculation and reduction of angles, yielding the outcomes showcased in tables 2 and 3.

**Table 2.** Horizontal Angles and Horizontal distances for P1 station.

| Backsight | Station | Foresight | Angle | Horizontal Distance (m) |
|---|---|---|---|---|
| P7 | P1 | P7 | 00°00’00.0” | 167.4939 |
| P7 | P1 | P2 | 00°00’34.0” | 8.3009 |
| P7 | P1 | P3 | 359°59’27.0” | 12.7380 |
| P7 | P1 | P4 | 359°59’10.5” | 45.8650 |
| P7 | P1 | P5 | 00°00’55.0” | 95.7540 |
| P7 | P1 | P6 | 00°00’14.0” | 135.2358 |

**Table 3.** Horizontal Angles and Horizontal distances for P7 station.

| Backsight | Station | Foresight | Angle | Horizontal Distance (m) |
|---|---|---|---|---|
| P1 | P7 | P1 | 00°00’00.0” | 167.4940 |
| P1 | P7 | P2 | 359°59’56.0” | 159.1939 |
| P1 | P7 | P3 | 00°00’01.5” | 154.7549 |
| P1 | P7 | P4 | 00°00’15.0” | 121.6287 |
| P1 | P7 | P5 | 359°58’45.5” | 71.7380 |
| P1 | P7 | P6 | 359°58’48.0” | 32.2569 |

Subsequently, using equation (1), the distances of pillars P2, P3, P4, P5, and P6 from the alignment formed by points P1 and P7 were calculated for each station. This process yielded two outcomes representing the misalignment of the pillars, facilitating a comparative analysis. The comparison involved subtracting the respective values, calculating their average, and estimating the standard deviation. All these details are presented in table 4.

**Table 4.** Result of misalignment.

| Point | ΔxP1 (m) | ΔxP7 (m) | dif (m) | media (m) | sd (m) |
|---|---|---|---|---|---|
| P2 | 0.00137 | 0.00309 | -0.00172 | 0.00223 | ±0.0002 |
| P3 | -0.00204 | -0.00113 | -0.00091 | -0.00159 | ±0.0007 |
| P4 | -0.01101 | -0.00885 | -0.00216 | -0.00993 | ±0.0017 |
| P5 | 0.02553 | 0.02591 | -0.00037 | 0.02572 | ±0.0027 |
| P6 | 0.00918 | 0.01126 | -0.00207 | 0.01022 | ±0.0036 |

Derived from the disparities in alignment among the pillars, as indicated in table 4, figure 4 was generated. This illustration geometrically represents the values obtained for the pillar positions, with an

exaggerated scale on the *y*-axis compared to the *x*-axis. Take note of the formation of a closed clockwise traverse, following the sequence: P1, P3, P4, P7, P6, P5, P2, P1.
The scale of the X axis is in tenths of a millimeter, so that the traverse could appear. If scales were used only in meters, the misalignments of the points in relation to the ordinate axis would not be visible, due to their smallness in relation to the distances between the pillars. This change in scale was made only so that the formation of the traverse could be clearly seen, and does not represent its real geometry, given that there is this difference in scale.

| | X (m e-4) | Y (m) |
|---|---|---|
| P1 | 0.0 | 0.0000 |
| P2 | 22.3 | 8.3009 |
| P3 | -15.9 | 12.7380 |
| P4 | -99.3 | 45.8650 |
| P5 | 257.2 | 95.7540 |
| P6 | 102.2 | 135.2358 |
| P7 | 0.0 | 167.4939 |

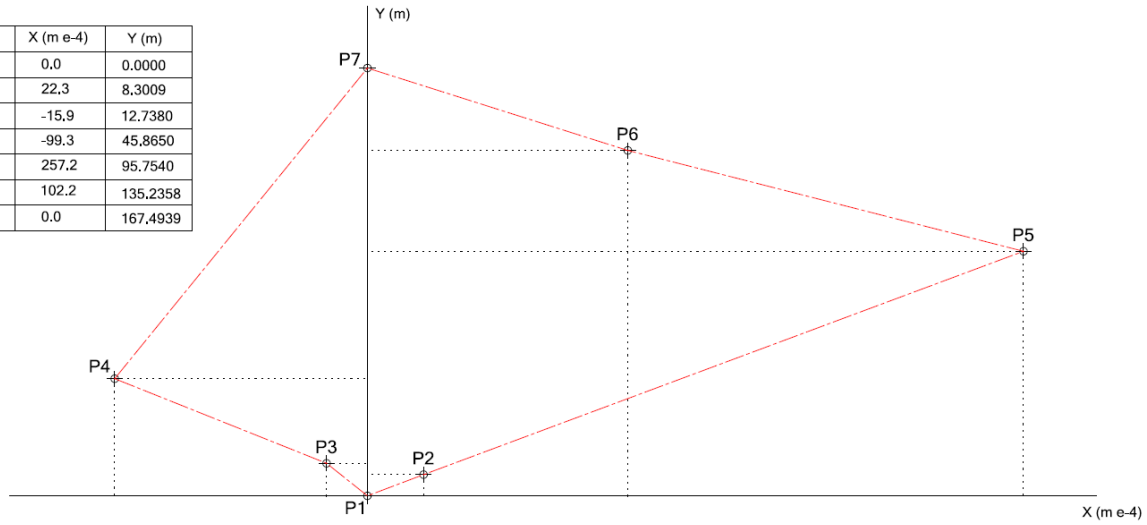


**Figure 4**. Misalignment of the pillars in relation to the alignment P1 P7.

## IV. CONCLUSIONS

A study on the alignment of the EDMI calibration baseline at The Federal University of Pernambuco was carried out. The results showed that, in relation to the alignment formed by pillars P1 and P7, all other pillars have some misalignment, however, only for three of them were found values greater than that relative to the nominal precision of the robotic total station used, which is ±2mm + 2ppm. Although the measurements reflected small misalignments between the pillars, due to its geometric configuration, the calibration base was presented in a way that can be treated as a traverse one, formed by the pillars P1, P3, P4, P7, P6, P5, P2, P1. This means that this traverse can be used as a reference for future monitoring of the pillars, because, if it is measured from time to time, and if new discrepancies are found, it means that there is a settlement that can be monitored through a time series, for example. Therefore, as future work, in addition to measuring the traverse, it is suggested that measurements be made using other equipment, such as precision GNSS receiver, and also the precision leveling of the pillars can be proposed, with a high precision level, so that the vertical misalignment can also be studied.

## ACKNOWLEDGEMENTS

The authors would like to thank the Department of Cartographic Engineering of the Federal University of Pernambuco, for providing the equipment and the technical infrastructure used for the acquisition of field data.

## REFERENCES

[1]. J. Uren, B. Price: Surveying for Engineers. Fifth edition. New York: Palgrave Macmillan, 2010.

[2]. N. W. J. Hazelton: Levelling and Total Stations. In: Surveying and Geomatics Engineering: principles, technologies, and applications, edited by D. T. Gillins, M. L. Dennis, A. Y. Reston: 2022. American Society of Civil Engineers, ASCE.

[3]. H. Simas, R. Di Gregorio, R. Simoni, M. Gatti: Parallel Pointing Systems Suitable for Robotic Total Stations: Selection, Dimensional Synthesis, and Accuracy Analysis. Machines 2024, 12, 54. https:// doi.org/10.3390/machines12010054.

[4]. I. da Silva: Geomatics Applied to Civil Engineering, State of the Art. In: J. K. Ghosh and I. da Silva (eds.): Applications of Geomatics in Civil Engineering, Lecture Notes in Civil Engineering 33. Springer Nature Singapore, 2020.

[5]. J. O. Ogundare: Precision Surveying: the principles and geomatics practice. Hoboken: John Wiley & Sons, 2016.

[6]. G. E. V. Becerra, R. A. Bennett, M. C. Chávez, M. E. T Soto, J. R. Camacho: Short Baseline Calibration using GPS and EDM Observations. Geofísica International 54-3: 255-266, 2015.

[7]. K. Daliga, Z. Kurałowicz: Examination method of the effect of the incidence angle of laser beam on distance measurement accuracy to surfaces with different color and roughness. Bol. Ciênc. Geod. Curitiba, v. 22, n°3, p.420-436, jul-set, 2016.

[8]. A. Geethalankara, A. Rupasinghe, N. C. Niriella: Studying the factors affect for the accuracy of reflectorless Total Station observations. Proceedings in Engineering, Built Environment and Spatial Sciences, 9th International Research Conference-KDU. Suriyawewa, p.325-330, 2016.

[9]. E. Lambrou: Modeling the Deviations of the Reflectorless Distance Measurement due to the Laser Beam's Incident Angle. International Journal of Applied Science and Technology. Online, v. 8, n. 1, p. 11-23, março, 2018.

[10]. Z. M. Zeidan, A. A. Beshr,; S. M. Sameh: Precision Comparison and Analysis of Reflectorless Total Station Observations. Mansoura Engineering Journal, (MEJ). Mansoura, v. 40, n°4, dez, 2015.

[11]. P. Holley, T. Perrine, T. Gamble: Is Reflectorless EDM Technology Reliable for Building Construction Layout Tolerances? Proceedings of 47th ASC Annual International Conference, Omaha, 6-9 April 2011.

[12]. H. S. Ali: An investigation into the Accuracy of Distance Measurements to an object with the Pulse (Non-Prism) Total Station. Sulaimani Journal for Engineering Sciences. Sulaimaniya, v. 03, n°03, p. 51-63, April, 2016.

[13]. S. I. Mohammed: Important methods measurements to exam the accuracy and reliability of reflectorless total station measurements. 2nd International Conference for Civil Engineering Science (ICCES 2021). Journal of Physics: Conference Series 1895 (2021). IOP Publishing.

[14]. C. J. Hope, S. W. Dawe: Precision survey monitoring with a reflectorless total station. FMGM 2015 – PM Dight (ed.). Australian Centre for Geomechanics. Perth, 2015.

[15]. S. Zakeri, S. Farzaneh: Measurement Methods for Cross-Sections of Tunnels Using Reflectorless Total Stations. Journal of the Earth and Space Physics, Vol. 46, n°4, p.93-101, winter 2021.

[16]. S. J. A. Garnés, A. Seixas, T. F. Silva: Análise do alinhamento da base de calibração multi pilar do LAMEP/UFPE com proposição de modelo de correção. V Simpósio Brasileiro de Ciências Geodésicas e Tecnologias da Geoinformação Recife - PE, 12- 14 de Novembro de 2014.

[17]. L. Nadolinetz, E. Levin, D. Akhmedov: Surveying Instruments and Technology. CRC Press. Boca Raton: 2017.

[18]. TOPCON: Instruction Manual - Geodetic Total Station GT series, 2022.

[19]. J. C. McCormack, W. A. Sarusa, W. J. Davis: Surveying, 6th Edition, 2012.

[20]. J. Kiusalaas: Numerical Methods in Engineering With Python 3. Cambridge University Press, Year: 2013.

[21]. H. Kahmen, W. Faig: Surveying. Berlin: de Gruyter, 1988.

[22]. C. D. Ghilani: Adjustment Computations: Spatial Data Analysis. Sixth edition. Hoboken: John Wiley & Sons, 2017.

[23]. J. O. Ogundare: Understanding least squares estimation and geomatics data analysis. Hoboken: John Wiley & Sons, 2019.

**AUTHORS**

**Isaac Ramos Junior** - Graduated in Surveying Engineering from Federal University of Viçosa, studying Master's in Geodetic Sciences and Geoinformation Technologies at Federal University of Pernambuco.

**Andrea de Seixas** is an Associate Professor at the Department of Cartographic Engineering at the Federal University of Pernambuco.

**Sílvio Jacks dos Anjos Garnés** has a Doctorate in Geodetic Sciences at Federal University of Paraná. He is an Associate Professor at the Department of Cartographic Engineering at the Federal University of Pernambuco.